

Report for NOAA/NGS

On:

Accuracy analysis of various NGS ionosphere estimation models

Dorota Grejner-Brzezinska, Pawel Wielgosz, Israel Kashani

Department Of Civil & Environmental Engineering & Geodetic Science
The Ohio State University
470 Hitchcock Hall, 2070 Neil Avenue, Columbus, OH 43210
Tel: 614-292-0169; Fax: 614-292-2957
Email: dbrzezinska@osu.edu
Email: kashani.1@osu.edu
Email: wielgosz.1@osu.edu

Submitted to
Dr. Gerald L. Mader
Chief, Geosciences Research Division
NOAA, National Geodetic Survey, N/NGS
1315 East-West Hwy.
Silver Spring, MD 20910-3282
Tel: 301-713-2854
Fax: 301-713-4475

July 9, 2004

Outline

In this report, a preliminary demonstration of the accuracy analysis of several methods of estimating the ionospheric corrections, based on reference GPS permanently tracking network, is presented. The ionospheric reference “truth” was selected as the double difference (DD) ionospheric correction, estimated from the dual frequency carrier phase data after fixing the DD ambiguities. The five ionospheric models that were tested are:

1. International GPS Service (IGS) global ionospheric map (GIM). IGS GIM is a combination of several different ionosphere models provided by IGS analysis centers (Schaer, 1999).
2. Absolute, smoothed pseudorange-based method – denoted as P4. For details, see Wielgosz et al. (2003)
3. Absolute carrier phase-based model, decomposed from double differenced ionospheric delays, denoted as MPGPS™. For details, see Kashani et al. (2004)
4. Absolute model based solely upon undifferenced dual frequency ambiguous carrier phase data – NGSa (Smith, 2004)
5. Carrier phase double difference-based tomographic method – NGSb (Spencer et al., 2004).

Methods 1-4 assume that the ionosphere is an infinitesimal single layer, while method 5 considers the ionosphere as a 3D layer.

The GPS data collected by the Ohio CORS stations — COLB and SIDN, on August 31, 2003, were selected for the analysis. The data were divided into two one-hour sessions. The first (night) session includes the data collected between 08:00–09:00 UT (3–4 am local time), when the total electron content (TEC) reached its daily minimum; the second (daytime) session, from the period 17:00–18:00 UT (1–2 pm local time), corresponds to the highest daily TEC level. This session allocation allows assessing the influence of varying ionospheric conditions on the model comparison results. The average PDOP was 2.9 during the night session and 3.9 during the daytime session (this would be relevant for the future positioning tests). The data-sampling interval was 30 seconds, and a total of 120 epochs per session were processed. The satellite elevation angles for the night-time and the day-time tests are plotted in figures 3 and 14, respectively.

Model 1 (GIM) provides absolute ionospheric delays in the IONEX format (grid). Thus, the ionospheric delays were interpolated for the user location using the linear interpolation. The Universal Kriging method was used to interpolate ionospheric delays provided by Models 2 (P4) and 3 (MPGPS™). Ionospheric delays in Model 4 (NGSa) were derived from the orthogonal function coefficients for the radial profiles, and in Model 5 (NGSb), the ionospheric delays were obtained directly from the phase measurement data used in this test. The corrections were provided to us as L1 absolute slant ionospheric delays (one value per satellite per epoch) in a modified RINEX format, so no interpolation was applied. It should be noted that NGSb model, at this point, includes only two DD, since the method is based on the trajectory cross-over, and no interpolation was applied to derive corrections for other satellites. Once this is available, similar analysis, but for the station position coordinates, will be carried out.

Results and Discussion

Example 1. 8:00-9:00 UT (night-time)

The analysis was performed on the baseline COLB-SIDN (104 km) as in shown in figure 1. The “truth” DD ionospheric delays are presented in figure 2 with the corresponding satellite elevation map in figure 3. Figures 4–13 represents the derived DD ionosphere from each method and the difference from the “truth” (in pairs). The mean and standard deviation of the ionospheric residuals from the “truth” are shown in Table 1.



Fig. 1 Baseline map

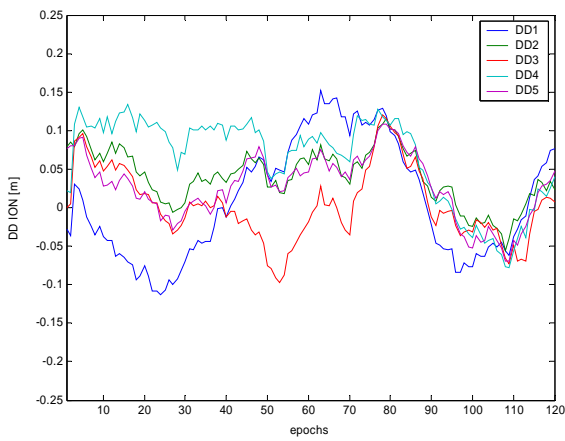


Fig. 2 "True" DD iono (night-time)

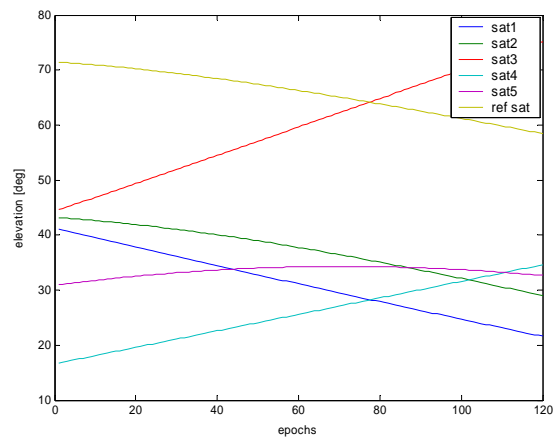


Fig. 3 Satellite elevations

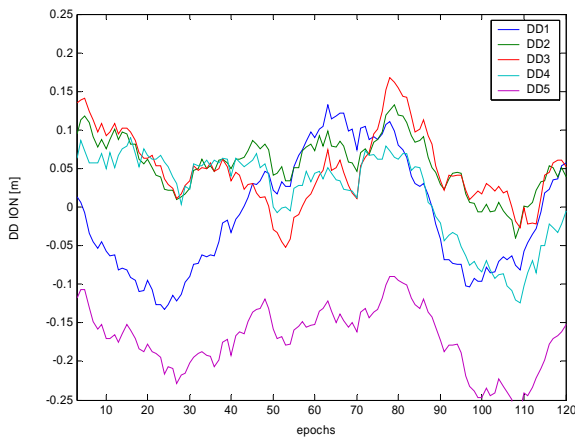


Fig. 4 P4 DD iono (night-time)

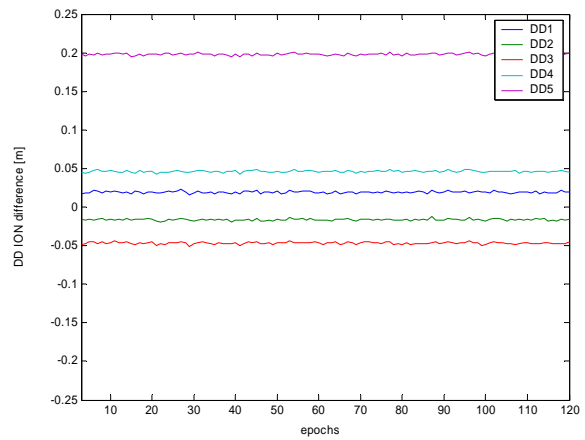


Fig. 5 P4 DD iono differences from the "truth" (night-time)

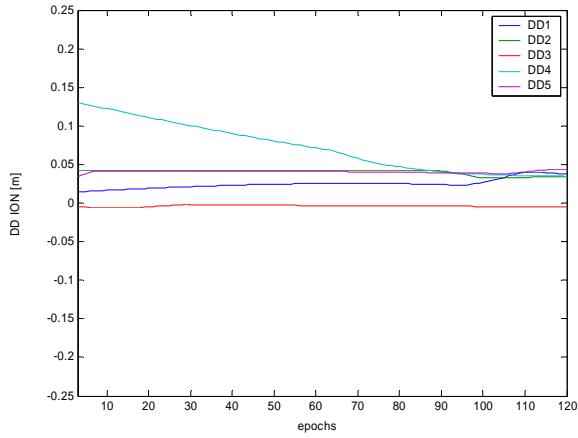


Fig. 6 GIM DD iono (night-time)

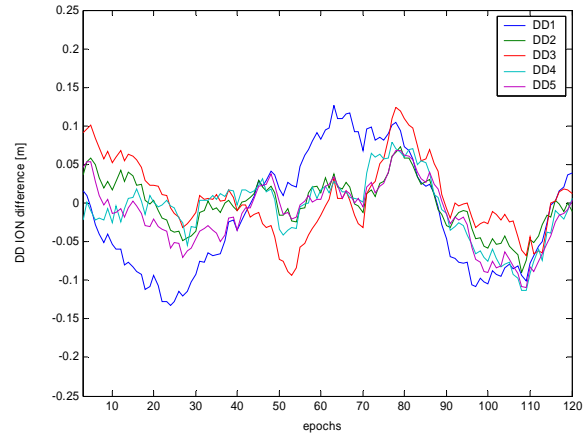


Fig. 7 GIM DD iono differences from the "truth" (night-time)

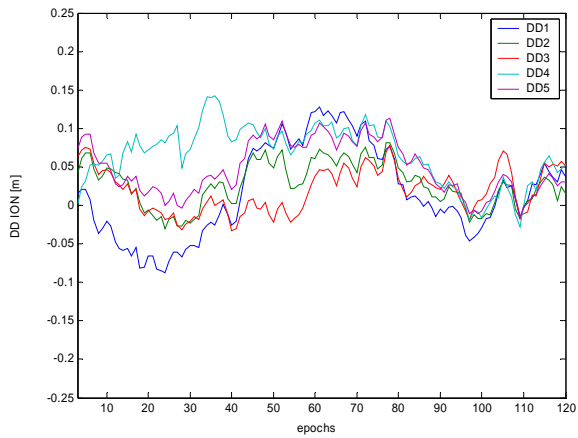


Fig. 8 MPGPS™ DD iono (night-time)

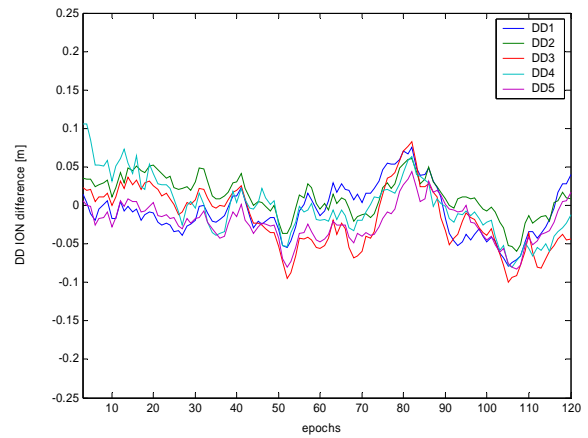


Fig. 9 MPGPS™ DD iono differences from the "truth" (night-time)

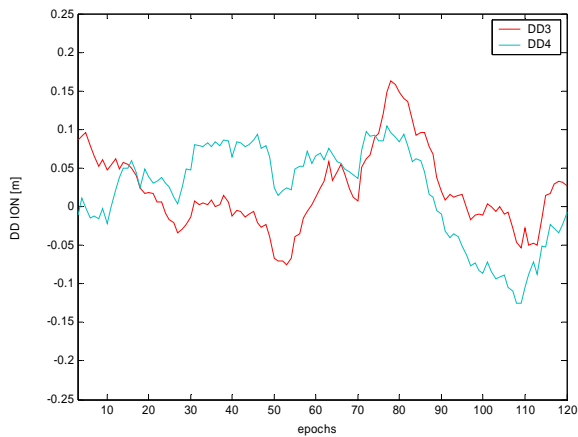


Fig. 10 NGSa DD iono (night-time)

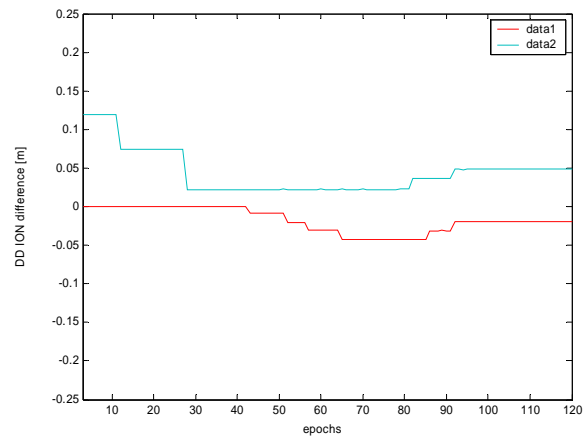


Fig. 11 NGSa DD iono differences from the "truth" (night-time)

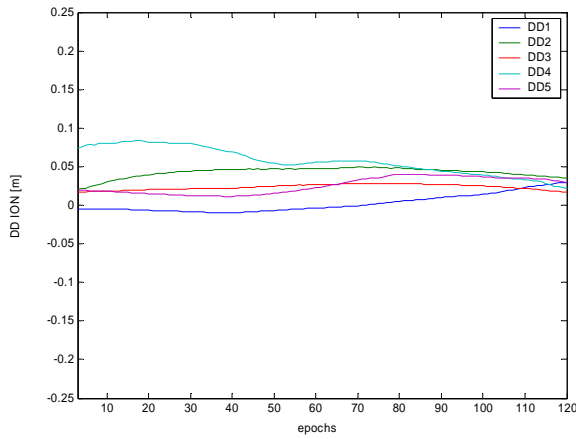


Fig. 12 NGSb DD iono (night-time)

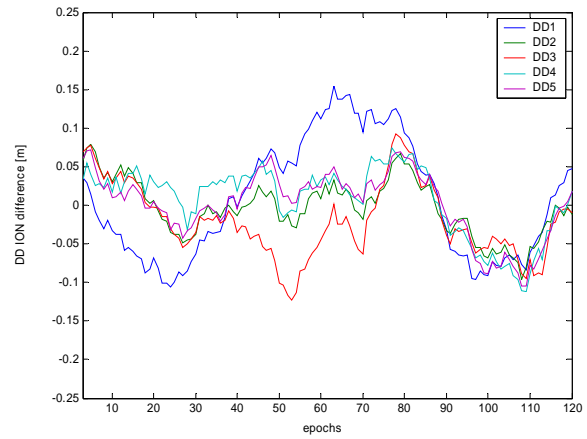


Fig. 13 NGSb DD iono differences from the “truth” (night-time)

Table 1. The mean and standard deviation (std) of the iono residuals from the “true” iono for all the methods (night time)

	PRNs	P4	GIM	MPGPS	NGSa	NGSb
mean [m]	24 - 4	0.02	-0.02	-0.01		0.01
	24 - 5	-0.02	-0.00	0.01		-0.00
	24-10	-0.05	0.01	-0.02	-0.02	-0.02
	24-17	0.05	-0.01	-0.00	0.04	0.01
	24-30	0.20	-0.01	-0.02		0.00
std [m]	24 - 4	0.00	0.07	0.03		0.08
	24 - 5	0.00	0.03	0.03		0.04
	24-10	0.00	0.05	0.04	0.02	0.05
	24-17	0.00	0.04	0.04	0.03	0.04
	24-30	0.00	0.04	0.03		0.04

Example 2. 17:00-18:00 UT (day-time)

The “truth” DD ionospheric delays are presented in figure 14 with the corresponding satellite elevation map in figure 15. Figures 16–25 represents the derived DD ionosphere from each method and the difference from the “truth” (in pairs). The mean and standard deviation of the ionospheric residuals from the “truth” are shown in Table 2.

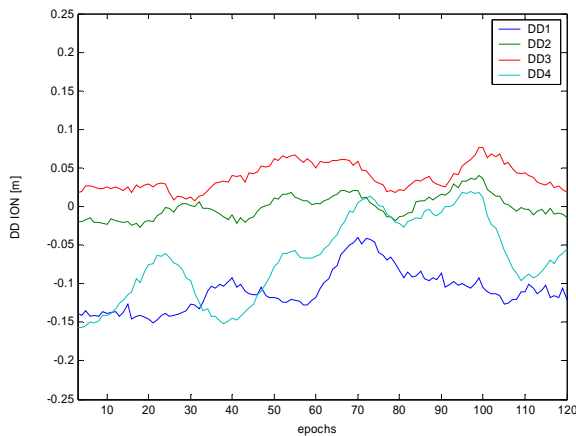


Fig. 14 “Truth” DD iono (day-time)

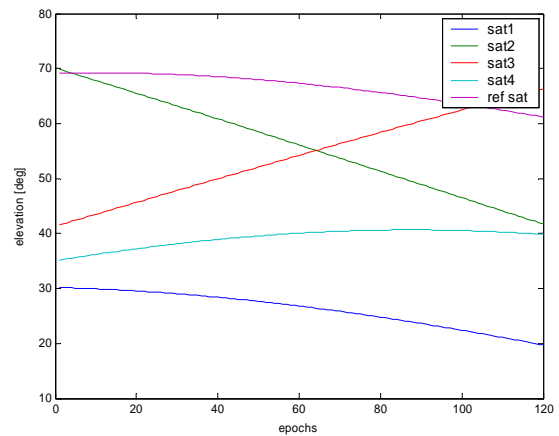


Fig. 15 Satellite elevations

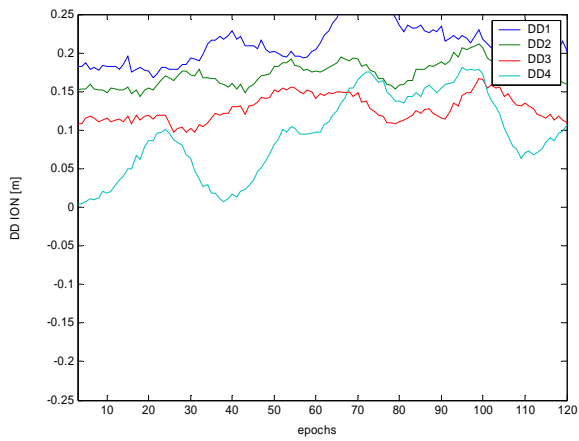


Fig. 16 P4 DD iono (day-time)

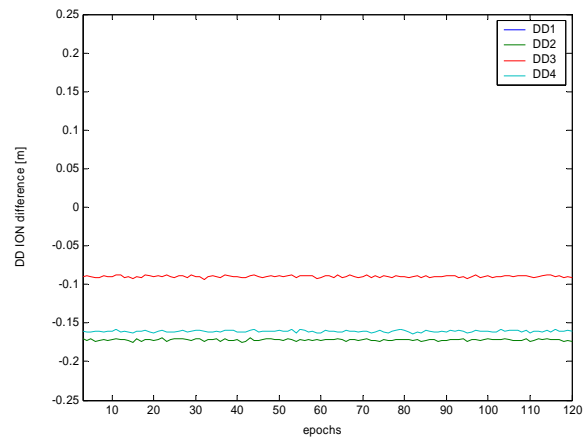


Fig. 17 P4 DD iono differences from the "truth" (day-time)

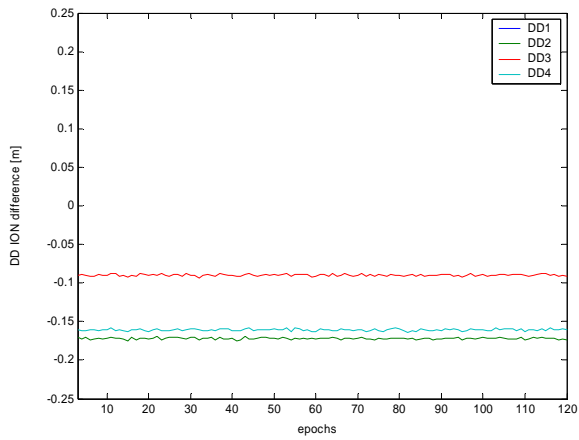


Fig. 18 GIM DD iono (day-time)

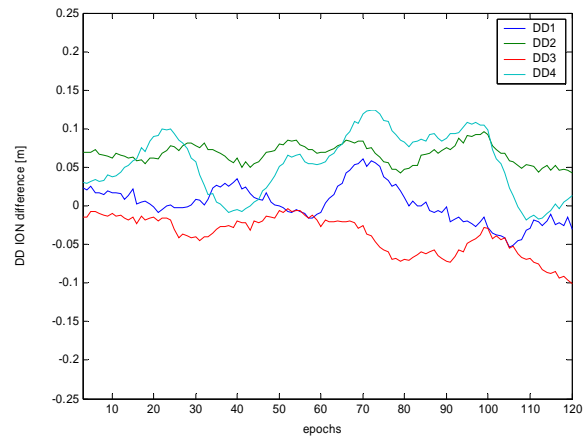


Fig. 19 GIM DD iono differences from the "truth" (day-time)

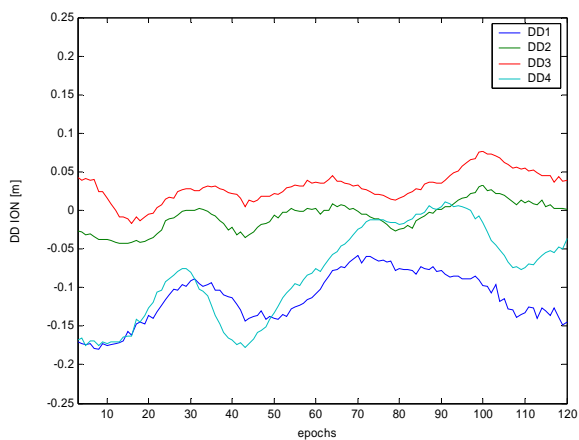


Fig. 20 MPGPS™ DD iono (day-time)

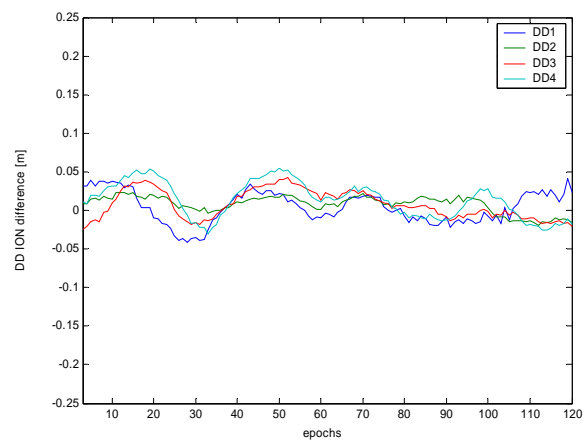


Fig. 21 MPGPS™ DD iono differences from the "truth" (day-time)

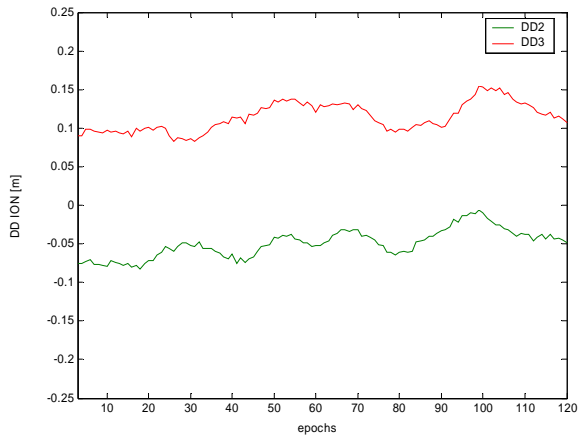


Fig. 22 NGSa DD iono (day-time)

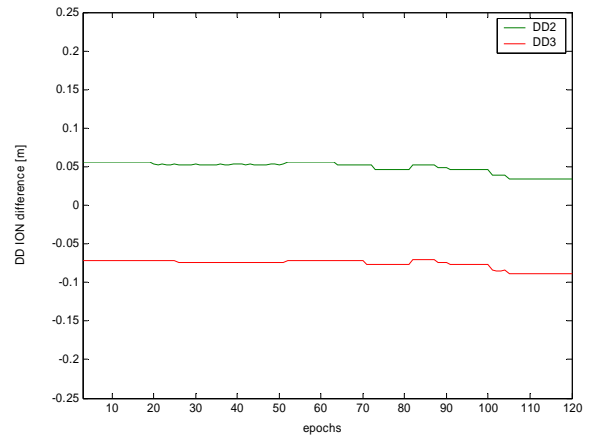


Fig. 23 NGSa DD iono differences from the "truth" (day-time)

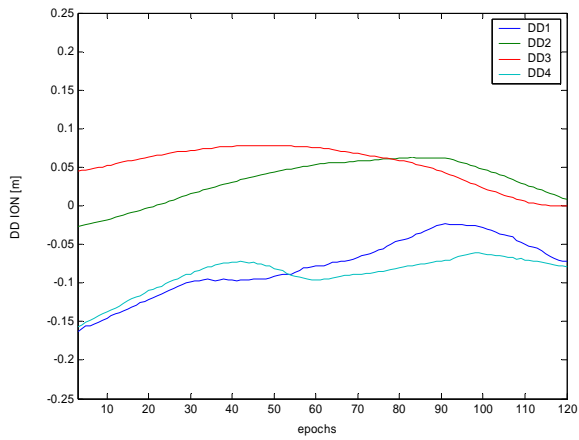


Fig. 24 NGSb DD iono (day-time)

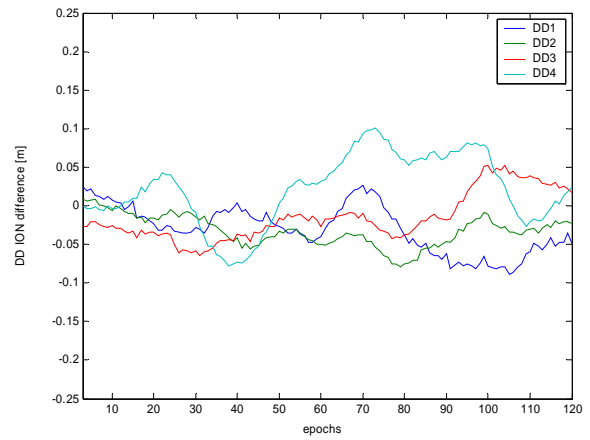


Fig. 25 NGSb DD iono differences from the "truth" (day-time)

Table 2. The mean and standard deviation (std) of the iono residuals from the "true" iono for all the methods (day-time)

	PRNs	P4	GIM	MPGPS	NGSa	NGSb
mean [m]	14 - 5	-0.32	0.00	0.00		-0.03
	14-23	-0.17	0.07	0.01	0.05	-0.03
	14-25	-0.09	-0.04	0.01	-0.08	-0.02
	14-30	-0.16	0.06	0.01		0.02
std [m]	14 - 5	0.00	0.02	0.02		0.03
	14-23	0.00	0.01	0.01	0.01	0.02
	14-25	0.00	0.02	0.02	0.01	0.03
	14-30	0.00	0.04	0.02		0.05

References

1. Grejner-Brzezinska, D.A., Kashani, I. and Wielgosz, P. (2004): Analysis of the Network Geometry and Station Separation for Network-Based RTK , Proceedings, ION NTM, San Diego, CA, January 26-28, CD ROM.
2. Kashani, I., Grejner-Brzezinska, D.A., and Wielgosz, P., (2004), Towards instantaneous RTK GPS over 100 km distances, Proceedings of ION 60th Annual Meeting, June 7-9, 2004, Dayton, Ohio (in print)
3. Schaer, S., Mapping and Predicting the Earth's Ionosphere Using the Global Positioning System, Ph.D. Thesis, Astronomical Institute, University of Berne, 205 pages, 1999
4. Smith, D.A. 2004: Computing unambiguous TEC and ionospheric delays using only carrier phase data from NOAA's CORS network. Proceedings of IEEE PLANS 2004, Monterey, California, April 26-29, 2004, pp. 527-537.
5. Spencer, P.S.J., D.S. Robertson and G.L. Mader, Ionospheric data assimilation methods for geodetic applications, Proceedings of the IEEE Position, Location and Navigation Symposium, Monterey, CA, 2004.
6. Wielgosz, P., Grejner-Brzezinska, D.A., and Kashani, I., (2003), Regional Ionosphere Mapping with Kriging and Multiquadric Methods, *Journal of Global Positioning Systems*, Vol. 2, Issue 1, pp. 48-55.